Bifurcation in a cw-pumped Brillouin fiber-ring laser: Coherent soliton morphogenesis

Carlos Montes, Abdellatif Mamhoud, and Eric Picholle

Laboratoire de Physique de la Matière Condensée, Centre National de la Recherche Scientifique, Université de Nice—Sophia Antipolis, Parc Valrose, F-06108 Nice Cedex 2, France

(Received 8 February 1993; revised manuscript received 8 October 1993)

Stability analysis allows the understanding of experimental steady and pulsed regimes observed in cw-pumped Brillouin fiber-ring lasers. The instantaneous acoustic response model proves to be singular, while the coherent stimulated-Brillouin-scattering (SBS) three-wave model yields a well-behaved Hopf bifurcation for a critical value of the feedback (several percent in intensity). The computed nonlinear dynamics shows self-organization of asymptotically stable Brillouin pulses, not depending on the initial noise. Further experiments support the bifurcation.

PACS number(s): 42.65.Es, 42.50.Rh, 42.60.Da, 47.20.Ky

I. INTRODUCTION

Recent observation of dissipative superluminous solitons in a Brillouin fiber-ring laser [1], whose nonlinear dynamics is well described by the one-dimensional (1D) coherent three-wave model of stimulated Brillouin scattering [2–5] (SBS), raises the question of the physical mechanism giving birth to such intense and short coherent structures in the backscattered Stokes wave, when the ring cavity is simply cw pumped. Ultracoherent cw Stokes output has been obtained for strong feedback [6], but with moderate coupling cw-pumped SBS resonators are essentially unstable [4]. It is known that both steady state and periodic oscillations may arise in a single-mode optical fiber with weak external feedback [7,8]. Steady, quasiperiodic, and even chaotic dynamics may take place when more than one cw pump beam is present [3]. Bursting oscillations and weak chaos can also be obtained for small enough feedback [9], but up to now no generic scenario has been proposed for the generation of asymptotically stable Brillouin pulses. We show in this paper that this stability is related to the finite material response time. The instantaneous acoustic response model yields a singularity due to the appearance of infinite frequency spectral components.

By using the coherent three-wave SBS model, we show here that a Hopf bifurcation takes place with the feedback R as the control parameter. For a given SBS gain, an initial condition-independent critical value R_{crit} separates two regimes: (i) above R_{crit} the cw-pumped system evolves towards the well-known steady "Brillouin mirror" regime [4,10], where monotonic backscattered amplification in the optical medium is saturated by the monotonic depletion of the forward propagating pump; (ii) below R_{crit}, self-organization of an asymptotically stable train of backward propagating "Brillouin solitons" [1] takes place. A morphogenesis scenario is shown in Fig. 1: The mirror regime becomes unstable for small enough feedback and the backscattered Stokes wave localizes into a soliton structure. Close to R_{crit}, both the steady and the pulsed regimes are reached after very long transients; this could account for the difficulty of their characterization, either numerical or experimental.

Within the "strong acoustic damping" approximation [10,11], Bar-Joseph *et al.* [7] performed a stability analysis for a line fiber cavity by perturbating the optical intensity equations. They showed that unstable oscillations appear for subcritical feedback and that relaxation oscillations occur in the stable domain. However, we shall see that this instantaneous response model breaks down at $R = R_{\mathrm{crit}}$ and is inappropriate to describe the finite amplitude oscillatory regime; it only allows energy transfer from the pump to the Stokes wave and may yield a singular evolution for the Brillouin pulse in the unstable regime by indefinitely growing its amplitude and shrinking its width [2]. At the bifurcation the infinite frequency mode becomes unstable, closely followed by all other cavity modes. This clearly violates the slowly varying envelope (SVE) approximation implicit in these models.

This anomaly is overcome in the three-wave model: Only the fundamental mode (of period neighboring the cavity transit time $n\mathrm{L}/c$) becomes unstable at the bifurcation; the higher harmonics are destabilized for lower values of R, with the fundamental mode still presenting the maximum growth rate. We obtain a well-behaved Hopf bifurcation suitable for a normal-form analysis [12]. In the nonlinear regime, anti-Stokes energy transfers are responsible for partial self-induced transparency: the generated Brillouin pulse saturates at a finite amplitude and width by transferring part of its trailing edge energy back to the pump, therefore propagating like a soliton [1,5].

II. STABILITY ANALYSIS

The nonlinear SBS process resonantly couples trough electrostriction a pump $E_p(\omega_p,\ k_p)$ and a backscattered Stokes $E_B(\omega_B,\ k_B)$ wave with an acoustic wave $E_a(\omega_a = \omega_p - \omega_B,\ k_a = k_p + k_B)$. Neglecting the acoustic propagation of speed $c_a \ll c$, one obtains within the SVE approximation three coupled SBS equations for the complex amplitudes [2-4]:

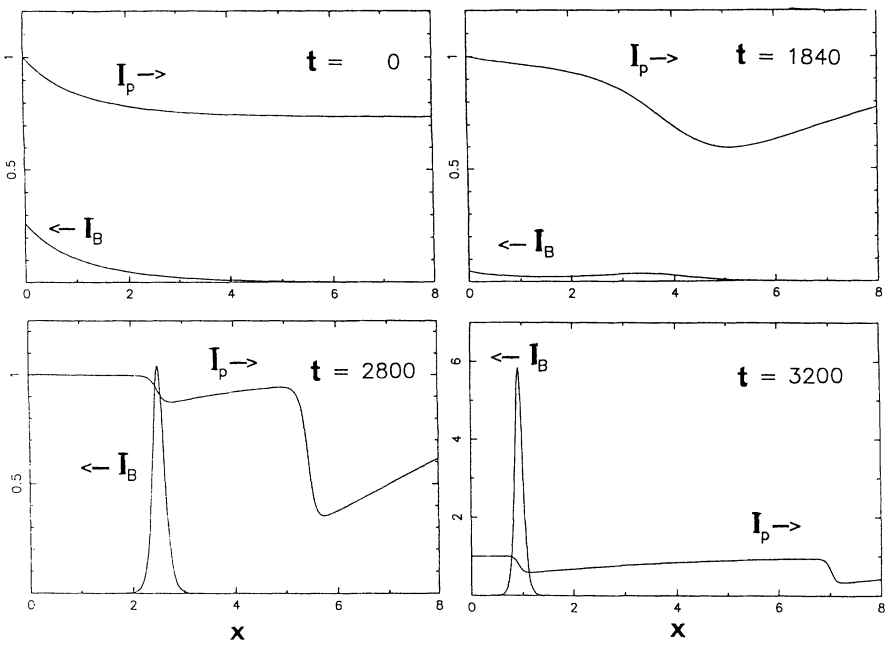

FIG. 1. Morphogenesis of the Brillouin soliton: For R below critical the steady SBS mirror becomes unstable and the system bifurcates towards the time dependent localized pulse regime for the backscattered Stokes wave (spatial distributions inside the optical medium at different times).

$$\left(\partial_t + \frac{c}{n}\partial_x + \gamma_e\right) E_p = -KE_BE_a,$$
$$\left(\partial_t - \frac{c}{n}\partial_x + \gamma_e\right) E_B = KE_pE_a^*,$$
$$(\partial_t + \gamma_a)E_a = KE_pE_B^*, \tag{1}$$

where γ_e (γ_a) is the damping coefficient for the optical (acoustic) waves and K is the SBS coupling constant [4] (cf. Table I).

The instantanous acoustic response model is obtained by neglecting the acoustical dynamics ($\partial_t E_a \ll \gamma_a E_a$) yielding the intensity equations

$$[\partial_x + (n/c)(\partial_t + 2\gamma_e)]I_p = -gI_pI_B,$$
$$[\partial_x - (n/c)(\partial_t + 2\gamma_e)]I_B = -gI_pI_B, \tag{2}$$

where $I_{p,B} = (n\epsilon_0 c/2)|E_{p,B}|^2$ and $g = 4K^2/(\gamma_a\epsilon_0 c^2)$ is the usual SBS gain coefficient [4].

We shall consider a cw-pumped fiber ring cavity of length L, in which the recoupling of the pump wave is avoided by an intracavity isolator. This device is independent of the recoupling phases [13]; the problem is reduced to one control parameter, namely, the Stokes intensity feedback efficiency $R = |\rho|^2 < 1$. The amplitude boundary conditions are

$$E_p(0,t) = E_{\rm cw}\ , \qquad E_B(L,t) = \rho E_B(0,t).$$

Here we will also study the stability of the oscillator by using the linear perturbative equations system around the nonlinear steady solution which is common to both systems (1) and (2), but now taking into account the finite time dependent acoustic response given by system (1). By defining the sum $2S = I_p + I_B$ and difference $2D = I_p - I_B$ variables in dimensionless units ($I_{p,B}/I_{\rm cw} \to I_{p,B}$, $xgI_{\rm cw} \to x$, $LgI_{\rm cw} \to \mathcal{L}$, and $tcgI_{\rm cw}/n \to t$), the steady-state solution without optical attenuation ($\gamma_e = 0$) reads

$$D = \text{const} \neq 0,$$
$$S(x) = D\frac{(S_0 + D)\exp(2Dx) + S_0 - D}{(S_0 + D)\exp(2Dx) - S_0 + D}\ , \tag{3}$$

and $S(x) = 1/[(1/S_0) + x]$ for $D = 0$. Inserting the boundary conditions [$S_0 = 1 - D$ and $S_L = R + (1 - 2R)D$] into Eq. (3), we obtain

$$R\exp(2D\mathcal{L}) = R + 2(1 - R)D. \tag{4}$$

The SBS laser threshold ($I_B = 0$, i.e., $2D = 1$) thus reads $R_{thd} = \exp(-\mathcal{L})$. Through $I_i(x,t) = I_i^{st}(x) + \delta I_i(x)\exp(-i\omega t)$ ($i = p, B, a$), where $I_a^{st} = I_p^{st}(x)I_B^{st}(x)/\mu^2$, $\mu = \gamma_a/KE_{\rm cw}$, and ω is the dimensionless complex eigenfrequency (defining instability for Im $\omega > 0$), the perturbative equations read

$$(-i\omega + \partial_x)\delta I_p = -f(\omega)\ \delta(I_pI_B),$$
$$(-i\omega - \partial_x)\delta I_B = f(\omega)\ \delta(I_pI_B), \tag{5}$$

with

$$f(\omega) = [1 - i(\omega/\mu^2)]/[1 - 2i(\omega/\mu^2)]$$

for the discrete set of frequencies (Re ω) which are solutions of the eigenvalue problem and define the longitudinal modes of the SBS ring cavity. For the fundamental mode $|\text{Re }\omega| \simeq 2\pi/\mathcal{L}$, we have $2|\text{Re }\omega|/\mu^2 = 2\pi c/(L\gamma_a n)$ ($\simeq \pi/100$ in our experiments [1,4]). The perturbative equations in the (S, D) variables read

$$i\omega\ \delta S = \partial_x \delta D, \tag{6a}$$
$$\partial_{xx}\delta D + 2S(x)f(\omega)\partial_x\delta D + [\omega^2 - 2if(\omega)\omega D]\delta D = 0, \tag{6b}$$

with the boundary conditions $\delta D(0) = -\delta S(0)$ and $\delta S(\mathcal{L}) - \delta D(\mathcal{L}) = 2R\delta S(0)$. Introducing in Eqs. (6) the variable change [14]

$$Y = (S_0 \sinh Dx + D \cosh Dx)^f \delta D$$

and $S(x)$ given in (3), Eq. (6b) becomes the complex eigenvalue equation

$$Y'' + [(\omega - ifD)^2 - f(1-f)(D^2 - S^2)]\, Y = 0. \qquad (7)$$

In the intensity approximation ($\omega/\mu^2 \to 0$), $f = 1$, and Eq. (7) is an harmonic oscillator equation of frequency $\Omega = \omega - iD$; the $(\delta I_p, \delta I_B)$ eigenmodes are easily calculated. Then, with the above boundary conditions, we find a characteristic equation for ω as function of R, D, and $\mathcal{L}$ [themselves related through Eq. (4)]:

$$A(\omega) + B(\omega) \sin \omega\mathcal{L} + C(\omega) \cos \omega\mathcal{L} = 0, \qquad (8)$$

where

$$A = 2\omega(\omega - iD),$$
$$B = 2i\omega^2 + b_1\omega + ib_2,$$
$$C = -2\omega^2 + ib_1\omega,$$
$$b_1 = -1 + R + 2D(2 - R),$$
$$b_2 = (1 - 2D)\big[R + 2D(1 - R)\big].$$

The marginal stability (Im $\omega = 0$) of the fundamental mode is shown in Fig. 2 where we plot $R_{\rm crit}$ as a function of the gain length $\mathcal{L}$ in curve (a) for this intensity model [yielding critical values close to those of the three-wave model, shown in curve (b)]. We plot in Fig. 3(a) the solutions in the complex ω plane, giving the growth (Im $\omega > 0$) and damping (Im $\omega < 0$) rates for different values of the feedback R and for a given gain length $\mathcal{L} = 8$. At the bifurcation ($R_{\rm crit} = 0.024\,28$) the highest frequency modes become unstable ($|\mathrm{Re}\ \omega| \to \infty$), and by decreasing R all the cavity modes ($|\mathrm{Re}\ \omega| = 2N\pi/\mathcal{L}$; N is an integer) become successively unstable down to the fundamental mode at $R = 0.021\,04$. The SVE approximation obviously breaks down. Nevertheless, this model gives simple estimations of the critical parameters, such as

$$D_{\rm crit} \simeq 1/6\ , \qquad R_{\rm crit} \simeq \left[3\exp(\mathcal{L}/3) - 2\right]^{-1}\ ,$$

through the singular relationships

$$\omega^2 = (2D^2 - D/2 + 1/4)(1 - 4D)/(6D - 1),$$
$$\omega \tan(\omega\mathcal{L}/2) = (1 - 4D)/2,$$

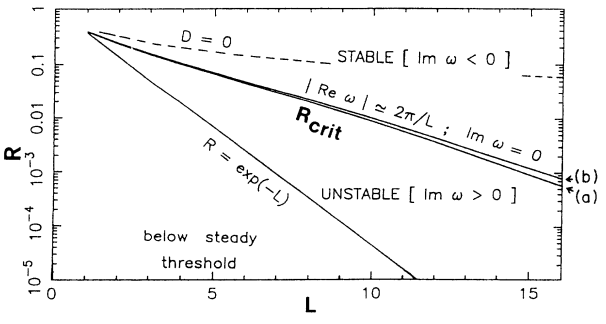

FIG. 2. Marginal stability of the fundamental mode: bifurcation curve [(a) intensity model and (b) three-wave model] separates stable and unstable domains in the $(R, \mathcal{L})$ plane.

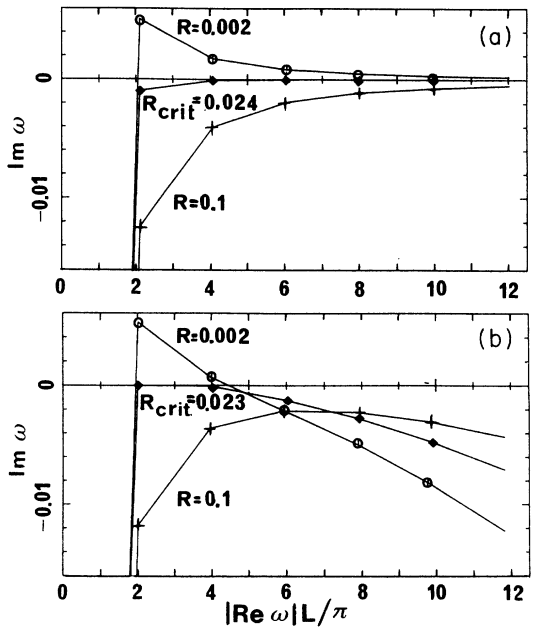

FIG. 3. Stability analysis: growth (damping) rate vs oscillation frequency for several R above and below critical: (a) intensity model, singularity ($|\mathrm{Re}\ \omega| \to \infty$) at $R = R_{\rm crit}$, (b) three-wave model, well behaved Hopf bifurcation of the fundamental mode $|\mathrm{Re}\ \omega|\mathcal{L} \simeq 2\pi$.

obtained from the complex Eq. (8) for Im $\omega = 0$ and $R \ll 1$. $R_{\rm crit}$ simply follows from Eq. (4) for $D_{\rm crit} \simeq 1/6$.

This high frequency divergency is overcome in the three-wave model, which introduces the finite acoustic response through the renormalization of ω by the complex factor $f(\omega)$. First of all, we have solved the eigenvalue problem of the harmonic oscillator with complex frequency $\Omega' = \omega - if(\omega)D$, by neglecting the potential term $f(1-f)(D^2 - S^2)$ in Eq. (7) [since $f(\omega) \simeq 1$]; this yields a characteristic equation similar to Eq. (8), depending on $f(\omega) = f_r(\omega) + if_i(\omega)$, where the coefficients have additional terms, namely,

$$A(\omega, f) = 2\omega(\omega - ifD)\ ,$$

$$B(\omega, f) = 2i\omega^2 + b_1\omega + if_ib_1\omega + ib_3 + b_4,$$

$$C(\omega, f) = -2\omega^2 - b_1f_i\omega + ib_1\omega\ ,$$

$$b_3 = (1 - f_i^2)b_2\ , \quad b_4 = -2f_ib_2.$$

The results show that the bifurcation is no longer singular [Fig. 3(b)]. Now, indeed, just under $R_{\rm crit}$ only the fundamental mode, which satisfies the SVE approximation, is unstable. For $\mathcal{L} = 8$ we obtain $R_{\rm crit} = 0.023\,20$, which is close to the critical value destabilizing the fundamental mode in the intensity model (Fig. 2), but here the higher modes are stable. Decreasing R, a small number of modes become unstable. This is numerically confirmed in the nonlinear regime, yielding asymptotically stable solitonlike pulses; its Fourier spectrum contains a finite number of modes [e.g., eight pairs in the case of Fig. 4(c)].

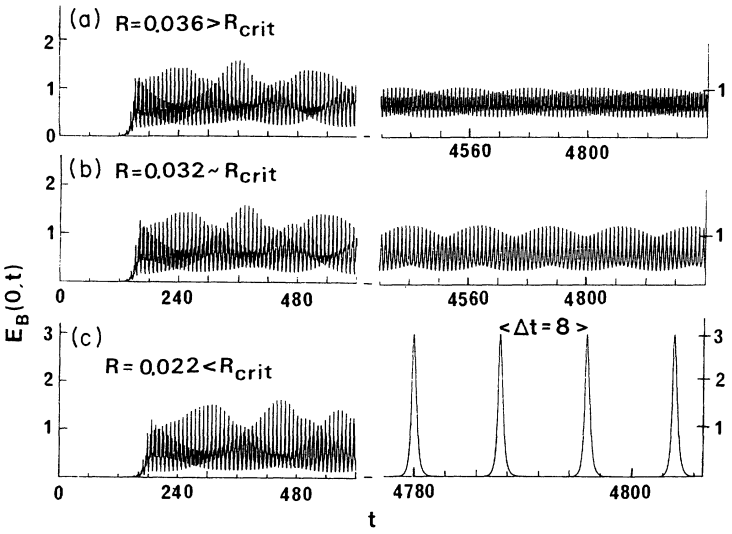

FIG. 4. Temporal behavior of the output Stokes $E_B(0,t)$ amplitudes solution of Eq. (1) [for $\mathcal{L} = LgI_{cw} = 8$, $\mu = 7$, and $\gamma_e/\gamma_a = 10^{-3}$]: (a) $R = 0.036 > R_{crit}$, evolution towards the mirror regime; (b) $R = 0.032 \sim R_{crit}$, longer transient near the bifurcation; (c) $R = 0.022 < R_{crit}$: solitonic morphogenesis (zoomed for the asymptotic side).

III. NUMERICAL THREE-WAVE DYNAMICS

For a given gain length $\mathcal{L}$, the Stokes feedback fully determines the two asymptotic states, starting from any initial noise conditions. The nonlinear dynamics governed by Eqs. (1) is shown in Fig. 4, for three feedback values around critical; R_{crit} is about 30% higher than the analytical value, due to the optical attenuation ($\gamma_e = 10^{-3}\gamma_a$) included in the numerical model. Starting from the same initial conditions (very small acoustic phase noise $E_a = 10^{-11}$ corresponding to thermal level), the three scenarios are hardly discernable during long transients (hundreds of round-trips). Above R_{crit} [Fig. 4(a)] the Stokes oscillations relax in amplitude, while the cw component grows until establishing the steady mirror regime. Near R_{crit} [Fig. 4(b)] the transients are extremely long. Below R_{crit} [Fig. 4(c)] the cw component tends to vanish in favor of stable solitonic pulses. We plot in Fig. 5 the mean asymptotic reflectivities obtained after long numerical simulation. It is interesting to note that, although the bifurcation causes a dramatic change in the mean amplitude of the backscattered wave, the mean energetic efficiency of SBS is the same in the two asymptotics.

We give in Table I the computation parameters for the cw-pumped Brillouin fiber-ring laser used in the numerical three-wave simulation. A laser pump power P corresponds to a flux intensity $I_p = P/S$, where S is an effective fiber cross section also depending on the overlap between its optical and acoustical modes. The fiber used here (pure SiO_2 core–borosilicate cladding) is acoustically antiguiding; the approximation $S = \pi r_{core}^2$ yields a severe overestimation of the SBS efficiency [15]. Therefore we must renormalize the SBS coupling constant K

TABLE I. Computation parameters for the cw pumped Brillouin fiber ring laser. The active medium is a single-mode fiber of length L= 80 m, with a 3-μm-diam core ($n_0 = 1.46$), an effective optical cross section $S = 7.2 \times 10^{-12}$ m^2, and an acoustical antiguiding factor $\sigma \simeq 3-4$. The pump wavelength is $\lambda = 514.5$ nm (acoustic wavelength $\lambda_a = 0.17$ μm). The coherent SBS coupling constant of Eqs. (1) is given by $K = \frac{1}{\sigma}(\varepsilon_0 c n_0^7/2\rho_0 c_a)^{1/2}(\pi p_{12}/\lambda) = (1/\sigma)$ 66 m s^{-1} V^{-1}. All parameters are given for $\sigma = 1$. P is the pump power coupled into the fiber, $I_p = P/S$ is the pump flux intensity, $\mathcal{L} = gLI_p$ is the dimensionless SBS intensity gain length [$g = 4K^2/(\gamma_a \varepsilon_0 c^2)$], E_p is the pump amplitude corresponding to $I_p = (n_0\varepsilon_0 c/2)|E_p|^2$, $\tau = (KE_p)^{-1}$ is the coherent SBS characteristic time, $\mu = \gamma_a\tau$ is the dimensionles acoustic damping rate ($\gamma_a = \pi\Delta\nu_B \simeq 5 \times 10^8 s^{-1}$), $\mu_e = \gamma_e\tau$ is the dimensionless optical damping rate ($\gamma_e \simeq 5 \times 10^5$ s^{-1}), (spatial intensity attenuation $\alpha = 2n_0\gamma_e/c = 21.7$ dB km^{-1}), and R_{crit} is the critical Stokes intensity feedback efficiency (for $\gamma_e = 0$).

P (mW)	10	20	30	40
I_p (MW/cm^2)	0.1	0.2	0.3	0.4
$\mathcal{L} = gLI_p$	4	8	12	16
E_p (MV/m)	0.75	1.06	1.29	1.50
$\tau = (KE_p)^{-1}$ (ns)	20.00	14.14	11.54	10.00
$\mu = \gamma_a\tau$	10.00	7.07	5.77	5.00
$\mu_e = \gamma_e\tau$	10^{-2}	7.07×10^{-3}	5.77×10^{-3}	5.0×10^{-3}
R_{crit}	0.11	2.3×10^{-2}	4.4×10^{-3}	7.9×10^{-4}

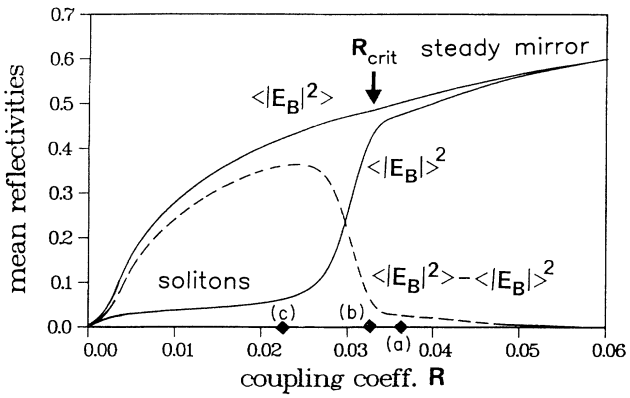

FIG. 5. Asymptotic mean reflected intensity, square mean amplitude and variance around the bifurcation (same gain $\mathcal{L} = 8$ as in Fig. 4). Feedback values (a)–(c) refer to Fig. 4.

by an acoustically antiguiding factor $1/\sigma < 1$ in order to obtain good agreement between numerical and experimental parameters; here $\sigma \simeq 3 - 4$.

IV. EXPERIMENT

In our experiment, R remains constant and the control parameter of the bifurcation becomes the power of the single-mode argon-ion ($\lambda = 514.5$ nm) cw-pump laser, or equivalently $\mathcal{L} = gLI_p$ (horizontal traveling in Fig. 2). The configuration is the basic Brillouin fiber-ring laser [4,16], with a 80-m-long polarization-maintaining single-mode fiber, closed trough two external beam splitters and an intracavity Faraday isolator ($R = 8\times10^{-3}$), and no external modulation (Fig. 6). High pump powers ($P > 400$ mW) yield a rather stable cw Stokes output [Fig. 7(a)]. High-frequency oscillations around the mirror [Fig. 7(b)] and large pulses coexist in the intermediate power range ($P \sim 350$ mW at the entrance of the fiber). A stable pulsed regime, slightly superluminous [1], is obtained for $P < 350$ mW [Fig. 7(c)]. For $R \simeq 4 \times 10^{-4}$, the device always present a stable pulsed behavior, up to $P \sim 1.5$ W.

In conclusion, due to the rather slow (ns) electrostrictive response, three-wave SBS interaction stands among the very few basic nonlinear and nonlocal physical processes in which the dynamics of the material response can be understood and experimentally characterized, thus explaining morphogenesis of large-scale coherent structures in a cw-pumped ring cavity, out of shapeless initial and boundary conditions. Moreover, this scenario is unchanged while taking into account the perturbative Kerr effect [4] and general recoupling conditions for both waves [17].

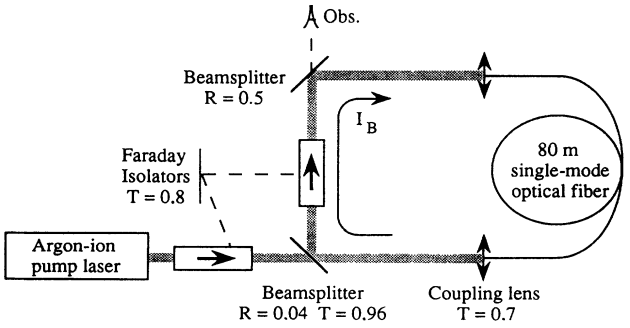

FIG. 6. Experimental setup.

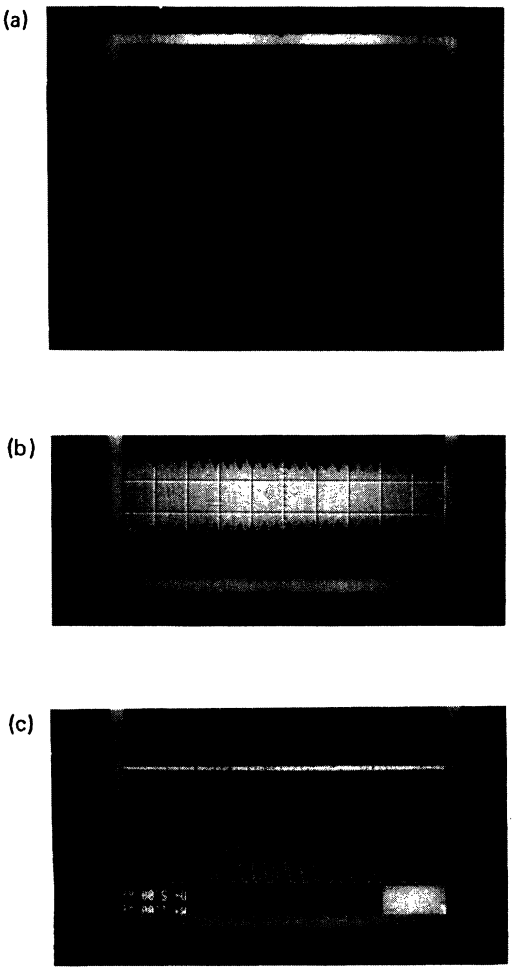

FIG. 7. Temporal structure of Stokes output for $R \simeq 8 \times 10^{-3}$ (experimental, 1 μs/div): (a) $P > 350$ mW, small amplitude fluctuations around the stable steady mirror; (b) $P \simeq 350$ mW large amplitude oscillations around the mirror; and (c) $P < 350$ mW, stable pulsed regime. The upper straight line gives the input pump level.

ACKNOWLEDGMENTS

We thank J. Botineau, J. Coste, A. Höök, D.J. Kaup, O. Legrand, C. Leycuras, F. Mortessagne, and A.M. Rubenchik. This work was supported by CNRS-Ultimatech.

[1] E. Picholle, C. Montes, C. Leycuras, O. Legrand, and J. Botineau, Phys. Rev. Lett. **66**, 1454 (1991).
[2] J. Coste and C. Montes, Phys. Rev. A **34**, 3940 (1986).
[3] C. Montes and J. Coste, Laser Part. Beams **5**, 405 (1987).
[4] J. Botineau, C. Leycuras, C. Montes, and E. Picholle, J. Opt. Soc. Am. B **6**, 300 (1989), and references therein.
[5] D.J. Kaup, J. Nonlinear Sci. **3**, 427 (1993).
[6] S.P. Smith, F. Zarinetchi, and S.E. Ezekiel, Opt. Lett. **16**, 393 (1991).
[7] I. Bar-Joseph, A.A. Friesem, E. Lichtman, and R.G. Waarts, J. Opt. Soc. Am. B **2**, 1606 (1985).
[8] A.L. Gaeta and R.W. Boyd, Internat. J. Nonlinear Opt. Phys. **1**, 581 (1992).
[9] R.G. Harrison, J.S. Uppal, A. Johnstone, and J.V. Moloney, Phys. Rev. Lett. **65**, 167 (1990).
[10] C.L. Tang, J. Appl. Phys. **37**, 2945 (1966).
[11] F. Chu and C. Karney, Phys. Fluids **20**, 1728 (1977).
[12] J.D. Crawford, Rev. Mod. Phys. **63**, 991 (1991).
[13] We have also characterized the bifurcation when both pump and Stokes waves are recoupled; $I_p(0)$ and $R_{\rm crit}$ then depend on the pump recoupling phase and efficiency. A moderate pump laser coherency causes a large unstable region around $R_{\rm crit}$. Reference [7] implies a quadrature relationship $[I_p(0) = I_{\rm cw} + RI_p(\mathcal{L})]$.
[14] C. Montes and J. Peyraud, in *Proceedings of the 288 Los Alamos Conference on Optics* (SPIE, Bellingham, WA, 1981), p. 199.
[15] C.K. Jen, J.E.B. Oliveira, N. Goto, and K. Abe, Electron. Lett. **24**, 1419 (1988).
[16] K.O. Hill, B.S. Kawasaki, and D.C. Johnson, Appl. Phys. Lett. **28**, 608 (1976).
[17] C. Montes, A. Mamhoud, and E. Picholle, *Nonlinear Coherent Structures in Physics and Biology*, edited by K.H. Spatschek and F.G. Maertens (Plenum, New York, 1993), pp. 351–356.

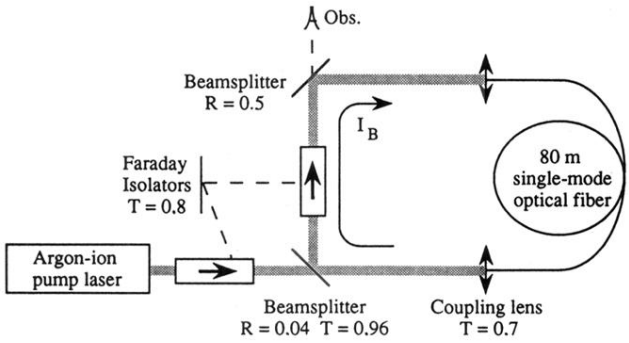

FIG. 6. **Experimental setup.**

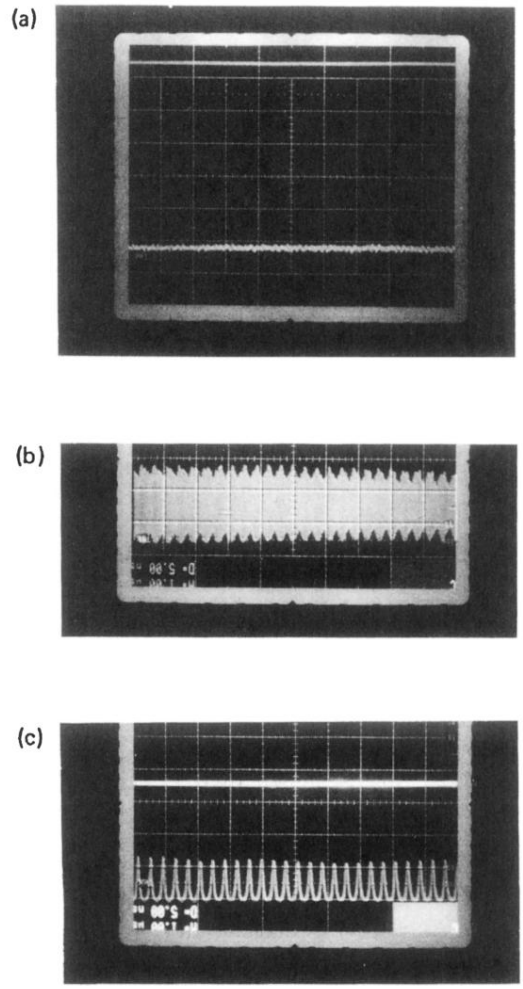

FIG. 7. Temporal structure of Stokes output for $R \simeq 8 \times 10^{-3}$ (experimental, 1 μs/div): (a) $P > 350$ mW, small amplitude fluctuations around the stable steady mirror; (b) $P \simeq 350$ mW large amplitude oscillations around the mirror; and (c) $P < 350$ mW, stable pulsed regime. The upper straight line gives the input pump level.